FULL PAPER DOI: 10.1002/adsc.201901230 Advanced Synthesis & Catalysis

Thermodynamic Reaction Control of Nucleoside Phosphorolysis

Felix Kaspar,[+a, b] Robert T. Giessmann,[+a] Peter Neubauer,[a] Anke Wagner,[a, b,*] and Matthias Gimpel[a]

[a] Bioprocess Engineering, Department of Biotechnology, Technische Universität Berlin, Ackerstraße 76, ACK24, D-13355 Berlin, Germany
Tel.: +49 30 314 72183
E-mail: anke.wagner@tu-berlin.de
[b] BioNukleo GmbH, Ackerstraße 76, D-13355 Berlin, Germany

[+] The authors contributed equally

Manuscript received: September 24, 2019; Revised manuscript received: November 15, 2019;
Version of record online: January 7, 2020

Supporting information for this article is available on the WWW under https://doi.org/10.1002/adsc.201901230

Abstract: Nucleoside analogs represent a class of important drugs for cancer and antiviral treatments. Nucleoside phosphorylases (NPases) catalyze the phosphorolysis of nucleosides and are widely employed for the synthesis of pentose-1-phosphates and nucleoside analogs, which are difficult to access via conventional synthetic methods. However, for the vast majority of nucleosides, it has been observed that either no or incomplete conversion of the starting materials is achieved in NPase-catalyzed reactions. For some substrates, it has been shown that these reactions are reversible equilibrium reactions that adhere to the law of mass action. In this contribution, we broadly demonstrate that nucleoside phosphorolysis is a thermodynamically controlled endothermic reaction that proceeds to a reaction equilibrium dictated by the substrate-specific equilibrium constant of phosphorolysis, irrespective of the type or amount of NPase used, as shown by several examples. Furthermore, we explored the temperature-dependency of nucleoside phosphorolysis equilibrium states and provide the apparent transformed reaction enthalpy and apparent transformed reaction entropy for 24 nucleosides, confirming that these conversions are thermodynamically controlled endothermic reactions. This data allows calculation of the Gibbs free energy and, consequently, the equilibrium constant of phosphorolysis at any given reaction temperature. Overall, our investigations revealed that pyrimidine nucleosides are generally more susceptible to phosphorolysis than purine nucleosides. The data disclosed in this work allow the accurate prediction of phosphorolysis or transglycosylation yields for a range of pyrimidine and purine nucleosides and thus serve to empower further research in the field of nucleoside biocatalysis.

Keywords: nucleosides; nucleoside phosphorylase; nucleoside phosphorolysis; equilibrium constant; temperature

Introduction

Nucleosides serve as drugs against a variety of cancers and viral infections.[1] Thus, their cost- and time-efficient preparation is of high interest. However, the synthesis of nucleosides and nucleoside analogs via conventional synthetic methods comes with several challenges posed by regio- and stereochemical complexity, functional group sensitivity and, consequently, heavy reliance on protecting groups.[2] Biocatalytic methods are a valuable alternative as pyrimidine and purine nucleosides can be synthesized with high selectivity in sustainable enzyme-catalyzed processes.[3] Here, the use of nucleoside phosphorylases (NPases) has been firmly established and these enzymes are widely applied for the synthesis of nucleosides and their analogues.[3]

NPases catalyze the phosphorolysis of nucleosides to pentose-1-phosphates, as well as the corresponding reverse reaction (Scheme 1). They are generally classified as either pyrimidine nucleoside phosphorylases

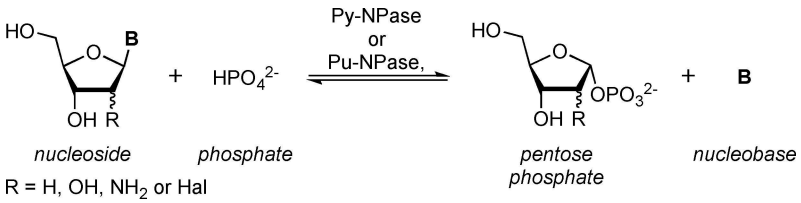

Scheme 1. Generalized biocatalytic nucleoside phosphorolysis reaction. A nucleoside is subjected to phosphorolytic cleavage of the nucleobase, yielding a pentose-1-phosphate and a free nucleobase.

(Py-NPases) or purine nucleoside phosphorylases (Pu-NPases), depending on their substrate spectra.[4]

The use of NPases as biocatalysts in organic chemistry offers the advantage of using mild aqueous reaction conditions, a broad substrate spectrum regarding sugar and base moieties, as well as perfect regio- and stereoselectivity at the C1' position. Employing these enzymes, pentose-1-phosphates can be obtained as important synthetic intermediates from the accessible pool of nucleosides[5,6] which have been shown to be highly valuable precursors for the synthesis of base- and sugar-modified nucleosides.[7–9] Furthermore, NPases are widely used for the synthesis of nucleoside analogues in transglycosylation reactions.[10–12]

Current research activities mainly focus on kinetic aspects of individual NPase-catalyzed reactions. Hence, kinetic data for a variety of NPases are available. To increase the final yield of phosphorolysis, mainly the choice of enzyme,[13,14] enzyme immobilization[15] or enzyme engineering[16,17] have been investigated. Nonetheless, NPases generally fail to facilitate full conversion.[18] A recent report by Alexeev and coworkers has shed more light on the cause of this phenomenon and showed that the thermodynamic properties of the nucleosides involved in the reaction influence the yields of NPase-catalyzed reactions.[19]

Since nucleoside phosphorolysis is a reversible reaction (Scheme 1), there is a point, where the rates of the forward and the backward reactions are equal and no apparent change in concentrations is observed. In this equilibrium state, the reaction quotient defined as the quotient of the concentrations of the products and the substrates can be derived from the law of mass action and is generally referred to as the apparent equilibrium constant K'.[20] The following expression results for nucleoside phosphorolysis reactions:

$$K' = \frac{[B][P1P]}{[N][P]} \quad (1)$$

where K' is the apparent equilibrium constant of phosphorolysis, $[B]$ is the equilibrium concentration of the free nucleobase [mM], $[P1P]$ is the equilibrium concentration of the pentose-1-phosphate [mM], $[N]$ is the equilibrium concentration of the nucleoside [mM] and $[P]$ is the equilibrium concentration of inorganic phosphate [mM].

This equilibrium constant exists irrespective of the (bio)catalyst used and K' values for some substrates in NPase-catalyzed reactions have been reported.[19,21–26] Thus, according to the law of mass action, only the reaction conditions influence the final equilibrium concentrations and not the enzyme used for catalysis. Alexeev and colleagues[19] recently employed this dependency in their method for accurate yield prediction of nucleoside transglycosylation reactions based on the equilibrium constants of the individual reactions. Ultimately, this allows for thermodynamic reaction control by adjusting the concentrations of the starting materials to facilitate an optimal yield.

In this work we provide extensive evidence for the universal interpretation of nucleoside phosphorolysis reactions as thermodynamically controlled endothermic equilibrium reactions that adhere to the law of mass action. To this end, we performed and monitored several biocatalytic nucleoside phosphorolysis reactions. We demonstrate that nucleoside phosphorolysis proceeds to a reaction equilibrium dictated by the substrate-specific equilibrium constant of phosphorolysis, irrespective of the type or amount of NPase used. Furthermore, we show that the equilibrium constant is temperature dependent. Therefore, we determined the equilibrium constants of phosphorolysis of 24 nucleosides at different temperatures and derived the apparent transformed enthalpies and entropies. The resulting data show that pyrimidine nucleosides are generally more susceptible to phosphorolysis than purine nucleosides. Additionally, our enthalpy and entropy data allow calculation of equilibrium constants at different temperatures as well as prediction of phosphorolysis yields, as demonstrated herein.

Results and Discussion

Maximum Conversions of Nucleosides in Phosphorolysis Reactions are Independent of the Applied Biocatalyst

Previous research activities have focused on the discovery of new enzymes[13,14] or enzyme immobilization strategies[15] to increase the obtained yield for

nucleoside phosphorolysis and transglycosylation reactions. Based on the thermodynamic characteristics of these reactions, however, we anticipated that the maximum conversion in phosphorolysis reactions would behave independently of the enzyme used.

To investigate the impact of different NPases on the equilibrium states of nucleoside phosphorolysis reactions, we initially performed the phosphorolysis of uridine (**1**) with *Escherichia coli* uridine phosphorylase (*E. coli* UP), *E. coli* thymidine phosphorylase (*E. coli* TP), *Bacillus subtilis* Py-NPase (*B. subtilis* Py-NPase) and two commercially available thermostable Py-NPases (Py-NPase Y01 and Py-NPase Y02). All enzymes readily accepted this substrate and reaction completion could be observed after 5 to 80 min using 10 $\mu g \cdot ml^{-1}$ of the respective enzymes (Figure 1A). Using 5 equivalents (eq.) of phosphate with respect to the nucleoside substrate, a maximum conversion of 55% was achieved regardless of the enzyme used.

To exclude any concentration effects of the enzyme preparations, we additionally conducted the phosphorolysis of **1** with different concentrations of Py-NPase Y02 (Figure 1B). Higher enzyme concentrations led to faster reaction completion. However, irrespective of the amount of the enzyme used, the same equilibrium as previously observed was reached.

To eliminate the possibility of enzyme inactivation preventing the completion of the reaction, we performed the phosphorolysis of **1** with Py-NPase Y02 and added additional enzyme after apparent reaction completion (Figure 1C).

This experiment resulted in no change of reactant concentrations after addition of more enzyme, confirming that this reaction was not terminated by means of inhibition and/or enzyme inactivation.

This evidence confirms that the phosphorolysis of uridine (**1**) is a thermodynamically controlled equilibrium reaction which is consistent with previous reports.[19,21–24,27] From the data collected, the apparent equilibrium constant of phosphorolysis K' under these conditions was 0.15, as calculated from equation (1).

To broadly confirm the thermodynamic reaction control of nucleoside phosphorolysis, we investigated the conversion of other nucleosides by NPases. We observed a similar behavior for the phosphorolysis of the pyrimidine nucleosides 2′-deoxyuridine (**2**), 5-fluorouridine (**3**) and 2′-deoxy-5-fluorouridine (**4**), employing the same Py-NPases (Figure 2A–2C). As observed for uridine (**1**), the choice of enzyme had no effect on the equilibrium conversions. Pyrimidines **2**–**4** displayed very similar apparent equilibrium constants to **1** (0.20 for **2**, 0.14 for **3** and **4**).

To extend this investigation to purine nucleosides, we performed the phosphorolysis of two natural (adenosine, **5**, and 2′-deoxyadenosine, **6**) and two modified purine nucleosides (2-chloroadenosine, **7**, and 2-chloro-2′-deoxyadenosine, **8**) with three different NPases (thermostable Pu-NPases N01 and N02 and *E. coli* Pu-NPase). Similar to the pyrimidine nucleosides mentioned above, the choice of the enzyme had no effect on the equilibrium concentrations of these reactions (Figure 2D–2G). Here, the equilibrium conversions with 5 eq. of phosphate were significantly lower, in the range of 20%. Calculation of the apparent equilibrium constants of phosphorolysis yielded values

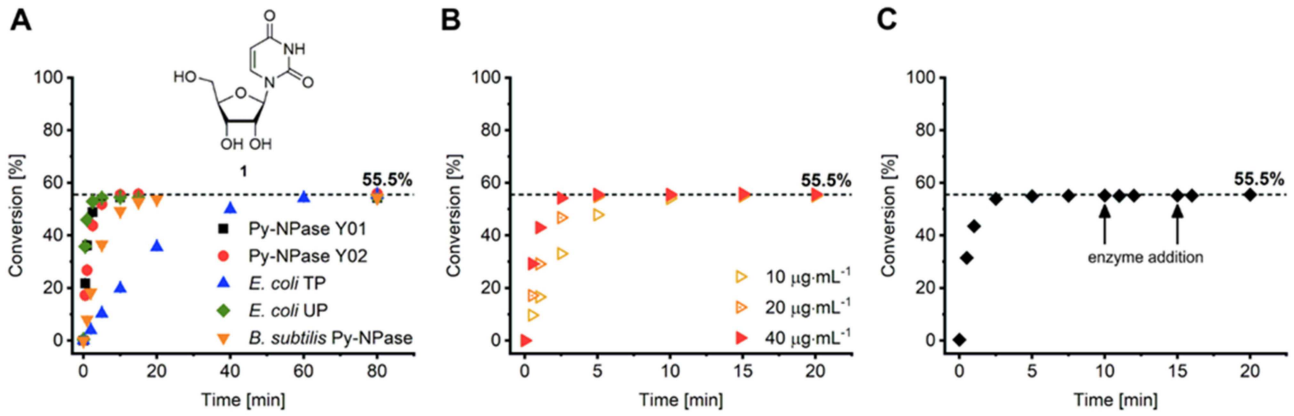

Figure 1. Enzymatic phosphorolysis of uridine (**1**). **A** Phosphorolysis of **1** with five different Py-NPases. **B** Phosphorolysis of **1** with Py-NPase Y02 using different enzyme concentrations. **C** Phosphorolysis of **1** with Py-NPase Y02 employing spiking of enzyme upon apparent reaction completion. All reactions reach the same equilibrium, regardless of the enzyme or its amount used for catalysis. Reactions were performed with 2 mM nucleoside substrate and 10 mM K_2HPO_4 in 50 mM MOPS buffer at pH 7.5 and 37 °C in a total volume of 500 µL. 10 $\mu g \cdot ml^{-1}$ of the respective enzyme were used in A and 10–40 $\mu g \cdot ml^{-1}$ Py-NPase Y02 were used in B. The reaction in C was started with 40 $\mu g \cdot ml^{-1}$ (20 µg total enzyme) Py-NPase Y02 and 10 µg of the enzyme were added at 10 min and 15 min each, indicated by the arrows. Reactions in A were performed in duplicate and the standard deviation (SD) is shown as error bars.

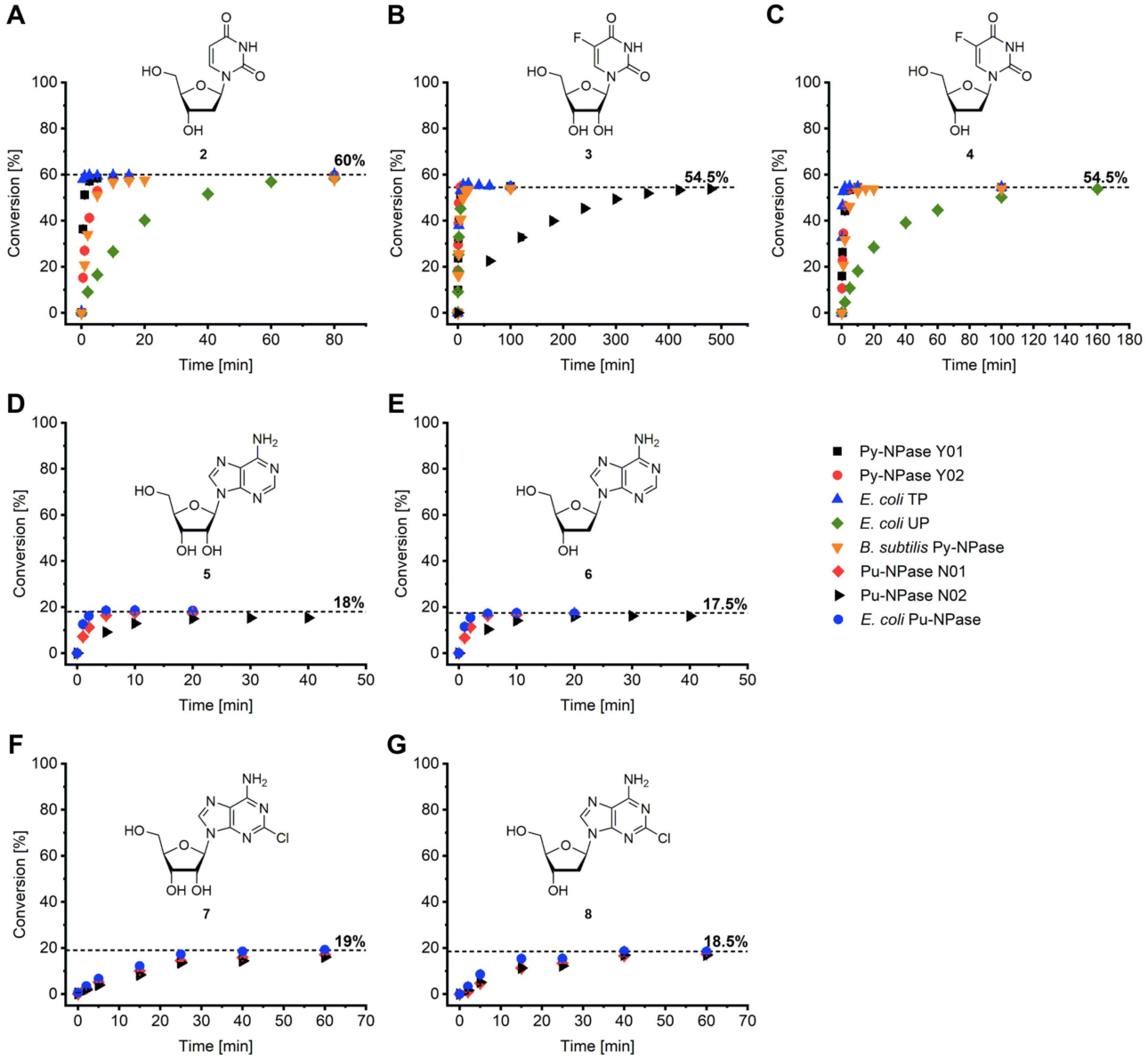

Figure 2. Enzymatic phosphorolysis of pyrimidine and purine nucleosides. The phosphorolysis of **A** 2′-deoxyuridine (**2**), **B** 5-fluorouridine (**3**), **C** 2′-deoxy-5-fluorouridine (**4**), **D** adenosine (**5**), **E** 2′-deoxyadenosine (**6**), **F** 2-chloroadenosine (**7**) and **G** 2-chloro-2′-deoxyadenosine (**8**) was performed in duplicate with 2 mM nucleoside substrate, 10 mM K_2HPO_4 and 10 $\mu g \cdot ml^{-1}$ of the respective enzyme (except for the phosphorolysis of **3** with Pu-NPase N02, where 600 $\mu g \cdot ml^{-1}$ were used) in 50 mM MOPS buffer at pH 7.5 and 37 °C in a total volume of 500 µL. Note the different time scales. Error bars show the SD.

around 0.01, which is consistent with previous reports for **5**.[19,28]

Interestingly, Py-NPases Y01, Y02 and *B. subtilis* Py-NPase performed roughly equally well with uridine (**1**) compared to 2′-deoxyuridine (**2**), whereas our data nicely reflect the inverse substrate specificity of *E. coli* UP and TP, as reported previously.[29,30] *E. coli* UP showed excellent activity with uridine (**1**) but significantly diminished activity with the 2′-deoxy analogue **2**. *E. coli* TP, on the other hand, displayed only low activity with **1** but facilitated remarkably quick reaction completion with **2** (Figure 1A and 2A).

Notably, although it is commonly believed that Pu-NPases should be specific to purine nucleosides, they generally also catalyze the phosphorolysis of pyrimidine nucleosides. Compared to corresponding Py-NPases they usually exhibit >2,000-fold lower turnover rates. Nonetheless, given the thermodynamic reaction control of nucleoside phosphorolysis, Pu-NPases should still be expected to complete the phosphorolysis of their unfavored substrates, despite

their kinetic handicap. Consequently, for the phosphorolysis of the pyrimidine 5-fluorouridine (**3**), even the use of the thermostable Pu-NPase N02 proved successful in reaching the thermodynamic equilibrium (Figure 2B). In this case, a 60-fold higher amount of enzyme had to be employed and the reaction took considerably longer than with any of the Py-NPases under the same reaction conditions. Thus far, to the best of our knowledge, only the phylogenetically peculiar *Plasmodium falciparum* Pu-NPase has been reported to perform the phosphorolysis of a pyrimidine nucleoside.[31] Here, we not only show for the first time that the thermostable Pu-NPase N02 accepts pyrimidine substrates such as **3**, but also achieves reaction completion given sufficient time. This strikingly emphasizes the non-significance of the enzyme kinetics for the ultimate reaction outcome, as it is possible to drive these phosphorolysis reactions into their chemical equilibrium even with an extremely small enzyme activity, in a range commonly considered negligible.

Thus, all nucleoside phosphorolysis reactions we investigated behaved according to the law of mass action and reached maximum product concentrations after a variable run time. Despite differences in reaction speed, the maximum conversion yields in the equilibrium are dictated by a characteristic and substrate-specific equilibrium constant which was shown to be independent of the type and amount of enzyme used. It may be reasonable to assume that this holds true for all nucleosides that are subjected to phosphorolysis. Important exceptions from this are nucleosides that are not converted by NPases because of issues such as excessive steric demands or severely unfavored transition states which prevent transformation.

Higher Reaction Temperature yields Higher Conversion of Nucleosides by NPases

The absolute values of the equilibrium constants of phosphorolysis of the nucleosides discussed above were all found to be well below 1. This means that they describe endothermic reactions, which are not favored under standard conditions. Consequently, we anticipated a temperature-dependence of K' and set out to investigate the effect of higher reaction temperatures on the equilibrium states of nucleoside phosphorolysis. Profiting from the use of the thermostable NPases Y02 and N02, we were able to perform the phosphorolysis of 24 nucleosides, including 12 pyrimidine and 12 purine nucleosides, at temperatures of 40 to 70 °C. To prevent decomposition of the produced pentose-1-phosphates, which is known to happen rapidly at high temperatures and neutral pH values,[5] we increased the reaction pH to 9. Under these conditions, both enzymes displayed excellent activity with all substrates **1**–**24** and allowed efficient reaction completion and monitoring. Consistent with our initial assumptions, we observed a trend towards higher conversions at higher temperatures. For example, under these conditions the phosphorolysis of 2′-deoxy-5-fluorouridine (**4**; Figure 3A) showed equilibrium conversions in the range of 51% at 40 °C and values around 55% at 70 °C. A similar behavior could be observed for all nucleosides investigated which confirms that the phosphorolysis of **1**–**24** are thermodynamically controlled endothermic reactions (Table S1).

The difference between the equilibrium conversions determined at pH 9 (this section) and the ones determined at pH 7.5 (see above) were insignificant (compare Figure 1 and Figure 2 with Table S1). Although a difference between them might be expected from the definition of the biochemical equilibrium, it seems that pH only minorly influences the equilibrium constant by changing the contribution of charged species.

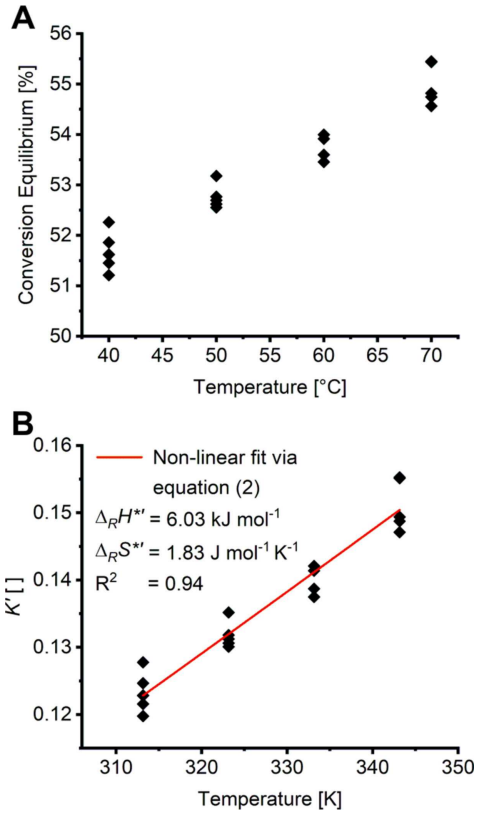

Figure 3. Examples of nucleoside phosphorolysis thermodynamic data processing. **A** Raw data of the phosphorolysis of **4** at different temperatures. The reactions were performed with 2 mM nucleoside substrate, 10 mM K_2HPO_4 and 16 µg·ml^{-1} Py-NPase Y02 in 50 mM glycine buffer at pH 9 and 40–70 °C in a total volume of 500 µL. **B** Transformed and fitted data for the derivation of $\Delta_R H'^*$ and $\Delta_R S'^*$. Raw data were processed via equation (1) and then fitted with equation (2).

Pyrimidine Nucleosides are Generally more Susceptible to Phosphorolysis than Purine Nucleosides

From the described data, we derived K' at various temperatures and determined the transformed apparent reaction enthalpy $\Delta_R H'^*$ and transformed apparent reaction entropy $\Delta_R S'^*$ via fitting of the data to:

$$K' = e^{-\frac{\Delta_R G'}{RT}} = e^{-\frac{\Delta_R H'^* - T\Delta_R S'^*}{RT}} \quad (2)$$

where $\Delta_R G'$ is the transformed apparent Gibb's free energy of phosphorolysis [$J \cdot mol^{-1}$], T is the temperature [K], R is the universal gas constant (8.314 $J \cdot mol^{-1} \cdot K^{-1}$), $\Delta_R H'^*$ is the transformed apparent enthalpy of phosphorolysis [$J \cdot mol^{-1}$], $\Delta_R S'^*$ is the transformed apparent entropy of phosphorolysis [$J \cdot mol^{-1} \cdot K^{-1}$], and the definitions from above.

Here, we carried out direct determinations through a non-linear fit to prevent error propagation by linearization (Figure 3A and 3B; see Table S1 for all derived values for $\Delta_R H'^*$ and $\Delta_R S'^*$; note that we communicate transformed thermodynamic values, as they were measured at constant pH and do not consider charged species, and explicitly abstain from referring to our results as "standard" values, but apparent ones, as they were not measured under standard biochemical conditions).

The knowledge of $\Delta_R H'^*$ and $\Delta_R S'^*$ then allowed access to the transformed apparent Gibb's free energy $\Delta_R G'$ of these phosphorolysis reactions at different temperatures. The Gibb's free energy of phosphorolysis $\Delta_R G'$ at 40 °C of pyrimidine nucleosides was found to be in the range of 1.2–5.5 $kJ \cdot mol^{-1}$, which is notably lower than for the investigated purine nucleosides that display values of 5.7–12.6 $kJ \cdot mol^{-1}$ (Figure 4A). These values correspond to apparent equilibrium constants K' in the range of 0.12–0.62 for pyrimidine nucleosides and 0.01–0.11 for purine nucleosides. Accordingly, noticeably different equilibrium conversions can be observed across these nucleosides, with pyrimidines generally featuring higher equilibrium conversions than purines, as dictated by their respective equilibrium constants (Figure 4B).

The practical value of our collection of $\Delta_R H'^*$ and $\Delta_R S'^*$ data lies within their use for the prediction of the equilibrium phosphorolysis conversion of the nucleosides investigated here. Using equation (2), the equilibrium constants of phosphorolysis of any of the nucleosides investigated here can easily be obtained for any given temperature. Employing then:

$$[B] = [P1P] = \frac{K'([N]_0 + [P]_0}{2(K'-1)} - \frac{\sqrt{(K'[N]_0 + K'[P]_0)^2 - 4(K'-1)K'[N]_0[P]_0}}{2(K'-1)} \quad (3)$$

where $[N]_0$ is the initial concentration of the nucleoside [mM], $[P]_0$ is the initial concentration of phosphate [mM] and definitions from above yields the concentrations of the free nucleobase and pentose-1-phosphate with variable initial concentrations of nucleoside and phosphate. Thus, conversions of these nucleosides can be predicted. To ease these calculations, we provided an Excel spreadsheet that is freely available from the externally hosted online supplementary material.[32]

To verify the predictions available through equation (3), we performed the NPase-catalyzed phosphorolysis of uridine (**1**) and adenosine (**5**) at pH 9 and 40 °C with different concentrations of phosphate (Figure 5). For example, pyrimidine **1** reached a conversion of 80% with 20 eq. of phosphate whereas for purine **5** we only observed a conversion of 37% under the same conditions, which is consistent with the predictions obtained via our collection of $\Delta_R H'^*$ and $\Delta_R S'^*$ data (Table S1). This emphasizes the practical value of the knowledge of the equilibrium constants of phosphorolysis of these nucleosides, as they allow for accurate prediction of phosphorolysis yields to optimize the reaction conditions.

Conclusion

In the present work, we broadly demonstrated that nucleoside phosphorolysis catalyzed by NPases is a thermodynamically controlled endothermic reversible equilibrium reaction. Therefore, maximum yields for each substrate are independent of the NPase used, as demonstrated by several examples, and can be predicted via the substrate-specific apparent equilibrium constant K'. We anticipate that this holds true for all nucleosides that can be subjected to phosphorolysis. Furthermore, we presented data on the temperature-dependency of the equilibrium constants of phosphorolysis of 24 nucleosides that display characteristic behavior. The available data allow for the calculation of K' at any given temperature and enable accurate prediction of phosphorolysis or transglycosylation yields for a range of pyrimidine and purine nucleosides.[33] Subsequently, the equations described by Alexeev *et al.*,[19] the thermodynamic data reported in this study, as well as the tools provided herein (see external supplementary material)[32] serve to facilitate streamlined reaction engineering of NPase-catalyzed reactions by *in silico* yield prediction and thermodynamic reaction control.[33]

Since our findings show that maximum yields in NPase-catalyzed reactions can be achieved independently of the enzyme applied, we believe that efforts to influence the yield of these reactions by varying the enzyme are unlikely to bear fruit. Instead, extending the toolbox of available NPases to improve kinetic parameters to reach reaction equilibrium faster or to

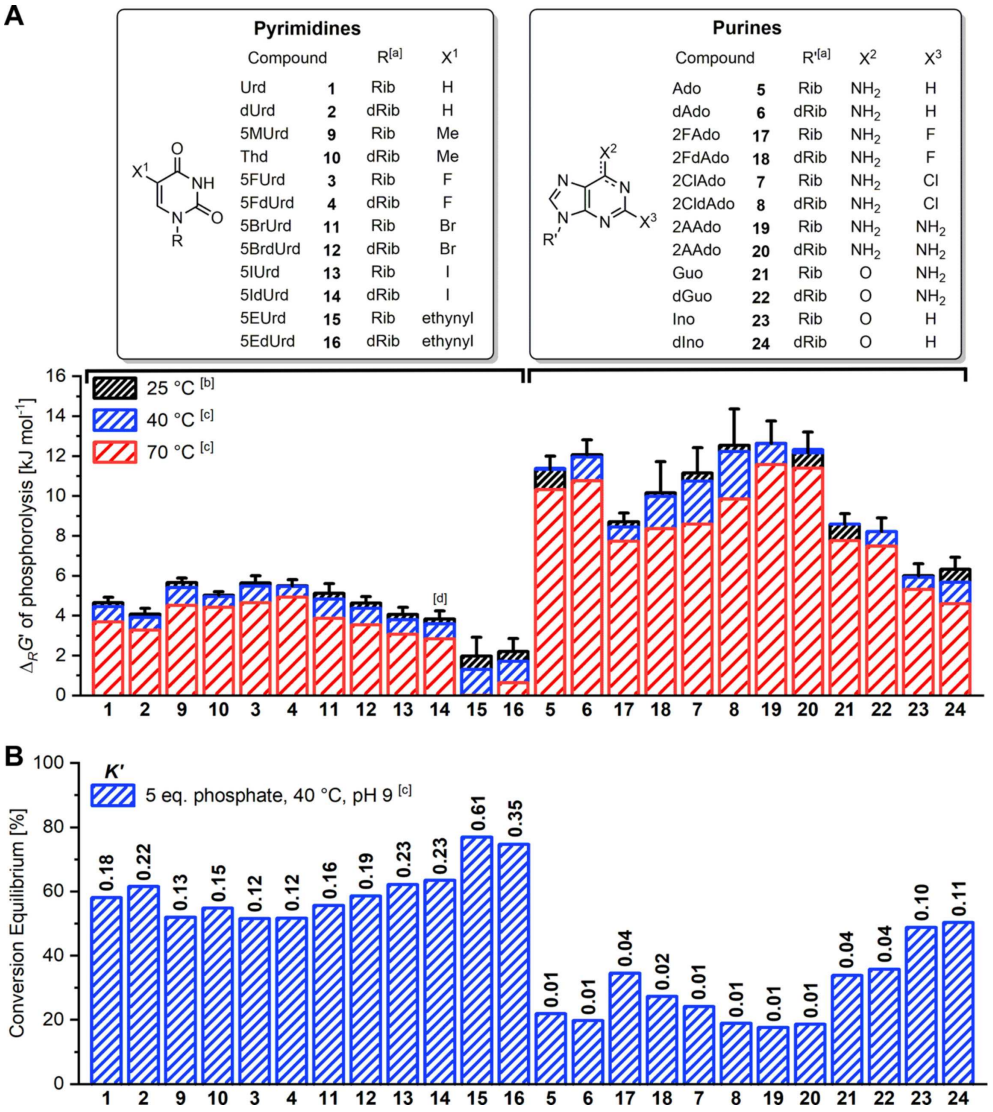

Figure 4. Gibb's free energy of phosphorolysis and conversion of nucleosides. **A** Gibb's free energy of phosphorolysis determined via equations (1) and (2) from the equilibrium concentrations of nucleoside phosphorolysis reactions with 2 mM nucleoside substrate, 10 mM K_2HPO_4 and 16 $\mu g \cdot ml^{-1}$ Py-NPase Y02 or 66 $\mu g \cdot ml^{-1}$ Pu-NPase N02 in 50 mM glycine buffer at pH 9 in a total volume of 500 µL performed at 40–70 °C. Error bars quantify the uncertainty of the prediction at 25 °C calculated via equation (4). **B** Equilibrium conversion of nucleosides in a phosphorolysis reaction at 40 °C and pH 9 employing 5 eq. of phosphate and equilibrium constant K' (also see Table S1). [a] Rib = ribosyl, dRib = 2′-deoxyribosyl, [b] extrapolated from experimental data for $\Delta_R H'^*$ and $\Delta_R S'^*$, [c] experimental data (conditions as above), [d] calculated from data for 50–70 °C since data for 40 °C were excluded from analysis (see Supplementary Material for full dataset).

convert challenging substrates such as arabinosyl nucleosides, fluorinated glycosides or bulky nucleobases will certainly prove beneficial.

Lastly, the quantification of effects of reaction conditions such as ionic strength, different salts, pH and chelating agents on the equilibrium states of nucleoside phosphorolysis may be explored experimentally by future studies.

Experimental Section

General Remarks

All chemicals were of analytical grade or higher and purchased, if not stated otherwise, from Sigma Aldrich (Steinheim, Germany), Carbosynth (Berkshire, UK), Carl Roth (Karlsruhe, Germany), TCI Deutschland (Eschborn, Germany) or VWR (Darmstadt, Germany). All nucleosides (Figure S1) and nucleobases were used without prior purification. Water deionized to 18.2 MΩ·cm with a Werner water purification system was used. For the preparation of NaOH solutions deionized water was used.

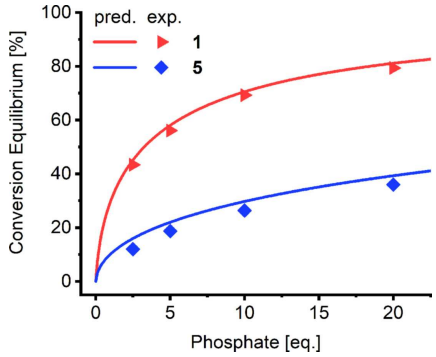

Figure 5. Predicted (pred.) and experimental (exp.) phosphorolytic conversion of uridine (**1**) and adenosine (**5**). Reactions were performed with 2 mM substrate and 5, 10, 20 or 40 mM (2.5, 5, 10 or 20 eq.) K_2HPO_4 and 40 μg·ml^{-1} Py-NPase Y02 or 40 μg·ml^{-1} Pu-NPase N02 in 50 mM glycine buffer at pH 9 and 40 °C in a total volume of 500 μL. Samples were taken after 10, 15 and 20 min to confirm equilibrium. The datapoints show the average of the three equilibrium data points. The predictions were calculated with equation (3) using K' (T) obtained through the $\Delta_R H'^*$ and $\Delta_R S'^*$ data for these substrates.

Enzymes

Enzymes were either purchased from BioNukleo GmbH (Berlin, Germany) or Sigma Aldrich (see Table S2). Enzymes provided by BioNukleo were E-PyNP-0001 (Py-NPase Y01; EC 2.4.2.2), E-PyNP-0002 (Py-NPase Y02; EC 2.4.2.2), E-PNP-0001 (Pu-NPase N01; EC 2.4.2.1), E-PNP-0002 (Pu-NPase N02; EC 2.4.2.1), E-UP-0001 (*Escherichia coli* uridine phosphorylase; *E. coli* UP; EC 2.4.2.3), E-TP-0001 (*E. coli* thymidine phosphorylase; *E. coli* TP; EC 2.4.2.4) and E-PNP-04 (*E. coli* purine nucleoside phosphorylase; *E. coli* Pu-NPase; EC 2.4.2.1). Enzymes were desalted against 2 mM KH_2PO_4 (pH 7.0, measured at 25 °C) buffer and stored at 4 °C at concentrations listed in Table S2. *Bacillus subtilis* pyrimidine phosphorylase (*B. subtilis* Py-NPase; EC 2.4.2.2) was obtained from Sigma Aldrich and prepared as a 1 mg·ml^{-1} solution in 2 mM KH_2PO_4 buffer (pH 7.5, measured at 25 °C) prior to use.

The activity of the stock solutions of Py-NPase Y02 and Pu-NPase N02 was assessed by the UV/Vis spectroscopy-based method described recently (also see below).[34] Reactions were performed with 1 mM of nucleoside substrate in 50 mM glycine buffer and 50 mM K_2HPO_4 at pH 9 and 40 °C. One unit (U) is defined as the conversion of 1 μmol of substrate per minute. For Py-NPase Y02 and Pu-NPase N02 an activity of 40 U·mg^{-1} (65 U·ml^{-1}) and 57 U·mg^{-1} (379 U·ml^{-1}) for their natural substrates uridine (**1**) and adenosine (**5**), respectively, was determined.

Phosphorolysis of Pyrimidine and Purine Nucleosides

Enzymatic nucleoside phosphorolysis reactions were prepared from stock solutions of nucleoside, phosphate, buffer and water in 1.5 mL reaction tubes (Sarstedt, Nümbrecht, Germany) and started by the addition of the enzyme. Reactions were performed in duplicate with 2 mM nucleoside and 10 mM K_2HPO_4 in 50 mM MOPS buffer (pH 7.5, measured at 30 °C) in a total volume of 500 μL. Prior to the addition of enzyme solution, reactions were preheated to 37 °C. Unless stated otherwise, final enzyme concentrations of 10 μg·ml^{-1} were used for all enzymes and substrates. For the phosphorolysis of 5-fluorouridine (**3**) with Pu-NPase N02, 600 μg·ml^{-1} of enzyme were employed.

To investigate possible effects of the enzyme concentration, uridine (**1**) was subjected to phosphorolysis using 10–40 μg·ml^{-1} of Py-NPase Y02. To exclude possible enzyme inactivation effects, **1** was also subjected to phosphorolysis with 40 μg·ml^{-1} of Py-NPase Y02 (20 μg total enzyme) and 10 μg of the enzyme were added after apparent reaction completion at 10 min and 15 min each. To validate the predictions of phosphorolysis conversion with different phosphate concentrations, 2 mM of **1** and **5**, respectively, were converted with 40 μg·ml^{-1} Py-NPase Y02 or 40 μg·ml^{-1} Pu-NPase N02 in 50 mM glycine buffer at pH 9 and 40 °C with 5, 10, 20 or 40 mM (2.5, 5, 10 or 20 eq.) K_2HPO_4. The reactions were monitored, and equilibrium samples were taken after 10, 15 and 20 min.

Monitoring of Enzyme Reactions

Sampling, data collection and analysis were carried out as described previously.[34] Briefly, samples of 30 μL (for pyrimidine nucleosides) or 20 μL (for purine nucleosides) were withdrawn from the reaction mixture and pipetted into 100 mM NaOH solution (200 mM NaOH solution for **3**, **4** and **13**–**16**) to give a final volume of 500 μL of diluted alkaline sample. From this mixture, 200 μL were pipetted into wells of a UV/Vis-transparent 96-well plate (UV-STAR F-Bottom #655801, Greiner Bio-One). The UV/Vis absorption spectra of these alkaline samples were recorded from 250 to 350 nm to determine the nucleoside/nucleobase ratio via spectra unmixing. All data presented in this study can be obtained from an external online repository[32] along with the software for spectral unmixing and metadata treatment detailed in our previous work.[34,35]

Temperature Dependence of the Equilibrium Constant

Equilibrium constants for the phosphorolysis of 24 nucleosides (**1**–**24**) were determined at pH 9 and at 40, 50, 60 and 70 °C. All reactions were performed with 2 mM nucleoside substrate and 10 mM K_2HPO_4 in 50 mM glycine buffer at pH 9. Unless stated otherwise, 16 μg·mL^{-1} (0.6 U·mL^{-1}) Py-NPase Y02 (for pyrimidine nucleosides) or 66 μg·mL^{-1} (3.7 U·mL^{-1}) Pu-NPase N02 (for purine nucleosides) were applied. For inosine (**23**) and 2′-deoxyinosine (**24**) 330 μg·mL^{-1} of Pu-NPase N02 were used and for 5-iodouridine (**13**) and 2′-deoxy-5-iodouridine (**14**) 32 μg·mL^{-1} of Py-NPase Y02. All reactions were performed in duplicate at temperatures from 40–70 °C in steps of 10 °C. Three samples were taken from each reaction once equilibrium was reached to confirm reaction completion. The time points used for sampling are given in Table S3. In total, 576 data points were recorded. Outliers that either displayed an elevated baseline due to UV absorption of the 96-well plate or differed

more than 1.5 percentage points from the other two data points within a sample set of a given temperature and reaction mixture were excluded from data interpretation. Consequently, 519 data points were considered for further evaluation. Data treatment and fitting was carried out with Origin ProLab 9. All data, as well as all subsequent calculations can be inspected as freely available data from an external online repository.[32] For each data point, K' was calculated via equation (1) and transformed apparent reaction enthalpy $\Delta_R H'^*$ [J·mol^{-1}] and transformed apparent reaction entropy $\Delta_R S'^*$ [J·mol^{-1}·K^{-1}] were fitted directly to all available datapoints for a substrate with equation (2). Similarly, $\Delta_R G'$ was calculated with equation (2) assuming that the apparent values $\Delta_R H'^*$ and $\Delta_R S'^*$ are independent of the reaction temperature in the considered range. The errors $\Delta\Delta_R H'^*$ [J·mol^{-1}], and $\Delta\Delta_R S'^*$ [J·mol^{-1}·K^{-1}] were derived from the fit and $\Delta\Delta_R G'$ was calculated via Gaussian error propagation:

$$\Delta\Delta_R G' = \sqrt{\Delta\Delta_R H'^{*2} + T^2 \Delta\Delta_R S'^{*2}} \quad (4)$$

with definitions from above.

Conflict of Interest

A.W. is CEO of the biotech company BioNukleo GmbH. F.K. is a researcher at BioNukleo GmbH and P. N. is a member of the advisory board.

Acknowledgements

We would like to thank Sarah von Westarp for her support with enzyme preparation, Niels Krausch for initial support with software development, and Dr. Erik Wade for revision of the manuscript. We are grateful for the support of R.T.G. by the German Research Foundation (DFG) under Germany's Excellence Strategy – EXC 2008/1 – 390540038 (UniSysCat), and by the Einstein Foundation Berlin (ESB) – Einstein Center of Catalysis (EC^2).

References

[1] L. P. Jordheim, D. Durantel, F. Zoulim, C. Dumontet, *Nat. Rev. Drug Discovery* **2013**, *12*, 447–464.
[2] J. Shelton, X. Lu, J. A. Hollenbaugh, J. H. Cho, F. Amblard, R. F. Schinazi, *Chem. Rev.* **2016**, *116*, 14379–14455.
[3] S. Kamel, H. Yehia, P. Neubauer, A. Wagner, in *Enzym. Chem. Synth. Nucleic Acid Deriv.*, **2019**, pp. 1–28.
[4] H. Yehia, S. Kamel, K. Paulick, A. Wagner, P. Neubauer, *Curr. Pharm. Des.* **2017**, *23*, 6913–6935.
[5] S. Kamel, M. Weiß, H. F. T. Klare, I. A. Mikhailopulo, P. Neubauer, A. Wagner, *Mol. Cancer* **2018**, *458*, 52–59.
[6] I. V. Kulikova, M. S. Drenichev, P. N. Solyev, C. S. Alexeev, S. N. Mikhailov, *Eur. J. Org. Chem.* **2019**, 6999–7004.
[7] I. V. Fateev, K. V. Antonov, I. D. Konstantinova, T. I. Muravyova, F. Seela, R. S. Esipov, A. I. Miroshnikov, I. A. Mikhailopulo, *Beilstein J. Org. Chem.* **2014**, *10*, 1657–1669.
[8] H. Komatsu, T. Araki, *Nucleosides Nucleotides Nucleic Acids* **2005**, *24*, 1127–1130.
[9] I. D. Konstantinova, K. V. Antonov, I. V. Fateev, A. I. Miroshnikov, V. A. Stepchenko, A. V. Baranovsky, I. A. Mikhailopulo, *Synthesis.* **2011**, 1555–1560.
[10] M. Rabuffetti, T. Bavaro, R. Semproli, G. Cattaneo, M. Massone, F. C. Morelli, G. Speranza, D. Ubiali, *Catalysts* **2019**, *9*, 355.
[11] B. Z. Eletskaya, D. A. Gruzdev, V. P. Krasnov, G. L. Levit, M. A. Kostromina, A. S. Paramonov, A. L. Kayushin, I. S. Muzyka, T. I. Muravyova, R. S. Esipov, *Chem. Biol. Drug Des.* **2019**, *93*, 605–616.
[12] X. Zhou, K. Szeker, B. Janocha, T. Böhme, D. Albrecht, I. A. Mikhailopulo, P. Neubauer, *FEBS J.* **2013**, *280*, 1475–1490.
[13] K. Szeker, X. Zhou, T. Schwab, A. Casanueva, D. Cowan, I. A. Mikhailopulo, P. Neubauer, *J. Mol. Catal. B* **2012**, *84*, 27–34.
[14] I. Serra, T. Bavaro, D. A. Cecchini, S. Daly, A. M. Albertini, M. Terreni, D. Ubiali, *J. Mol. Catal. B* **2013**, *95*, 16–22.
[15] D. F. Visser, F. Hennessy, J. Rashamuse, B. Pletschke, D. Brady, *J. Mol. Catal. B* **2011**, *68*, 279–285.
[16] D. P. Nannemann, K. W. Kaufmann, J. Meiler, B. O. Bachmann, *Protein Eng. Des. Sel.* **2010**, *23*, 607–616.
[17] X. Xie, W. Huo, J. Xia, Q. Xu, N. Chen, *Enzyme Microb. Technol.* **2012**, *51*, 59–65.
[18] R. T. Giessmann, N. Krausch, F. Kaspar, N. M. Cruz Bournazou, A. Wagner, P. Neubauer, M. Gimpel, *Process* **2019**, *7*, 380.
[19] C. S. Alexeev, I. V. Kulikova, S. Gavryushov, V. I. Tararov, S. N. Mikhailov, *Adv. Synth. Catal.* **2018**, *360*, 3090–3096.
[20] IUPAC, *Compendium of Chemical Terminology*, Blackwell Scientific Publications, Oxford, **1997**.
[21] N. G. Panova, E. V. Shcheveleva, C. S. Alexeev, V. G. Mukhortov, A. N. Zuev, S. N. Mikhailov, R. S. Esipov, D. V. Chuvikovsky, A. I. Miroshnikov, *Mol. Biol.* **2004**, *38*, 770–776.
[22] R. A. Alberty, *Biophys. Chem.* **2007**, *127*, 91–96.
[23] A. Vita, C. Y. Huang, G. Magni, *Arch. Biochem. Biophys.* **1983**, *226*, 687–692.
[24] R. Bose, E. W. Yamada, *Biochemistry* **1974**, *13*, 2051–2056.
[25] R. A. Alberty, *J. Chem. Thermodyn.* **2004**, *36*, 593–601.
[26] R. N. Goldberg, Y. B. Tewari, T. N. Bhat, *J. Phys. Chem. Ref. Data* **2007**, *4*, 1347–1397.
[27] T. A. Krenitsky, G. W. Koszalka, J. V. Tuttle, *Biochemistry* **1981**, *20*, 3615–3621.
[28] M. Camici, F. Sgarrella, P. L. Ipata, U. Mura, *Arch. Biochem. Biophys.* **1980**, *205*, 191–197.
[29] A. Hatano, A. Harano, Y. Takigawa, Y. Naramoto, K. Toda, Y. Nakagomi, H. Yamada, *Bioorg. Med. Chem.* **2008**, *16*, 3866–3870.
[30] J. C. Leer, K. Hammer-Jespersen, M. Schwartz, *Eur. J. Biochem.* **1977**, *75*, 217–224.

[31] G. A. Kicska, P. C. Tyler, G. B. Evans, R. H. Furneaux, K. Kim, V. L. Schramm, *J. Biol. Chem.* **2002**, *277*, 3219–3225.
[32] F. Kaspar, R. T. Giessmann, **2019**, 10.5281/zenodo.3530526
[33] F. Kaspar, R. T. Giessmann, K. Hellendahl, P. Neubauer, A. Wagner, M. Gimpel, ChemBioChem, in press.
[34] F. Kaspar, R. T. Giessmann, N. Krausch, P. Neubauer, A. Wagner, M. Gimpel, *Methods Protoc.* **2019**, *2*, 60.
[35] R. T. Giessmann, N. Krausch, **2019**, 10.5281/zenodo.3243376.

biocat2020
HAMBURG

10th INTERNATIONAL CONGRESS ON BIOCATALYSIS

30 AUG–03 SEP 2020

HAMBURG UNIVERSITY OF TECHNOLOGY | GERMANY

MAJOR TOPICS

- Computational analysis for enzyme discovery and design
- Structure-function analysis and enzyme optimization
- Enzymatic and whole-cell biotransformation
- Bioprocess engineering and enzyme application
- Sustainable industrial processes, biorefinery and bioeconomy

Abstract deadline 20 March 2020

www.biocat-conference.de

conventus
CONGRESSMANAGEMENT